29th International Conference
ENGINEERING MECHANICS 2023
Milovy, Czech Republic, May 9 – 11, 2023

NUMERICAL SIMULATIONS OF PLANE STRAIN TENSION FOR NICKEL-BASED ALLOY 718

Kubík P.*, Vobejda R., Petruška J.***, Šebek F.******

Abstract: *The analysis of possible approaches to the numerical simulation of tensile flat specimen made from 718 superalloy is presented. Three plasticity models were employed, with various numbers of material parameters and, therefore, complexity. The influence of simplifying the three-dimensional geometry into the plane was researched in the view of force response, deformation and stress state in the crack initiation location, which was in the centre of the specimen.*

Keywords: Ductile, Flow, Haynes, Inconel, Isotropic.

1. Introduction

The correct description of the deformation, stress state and failure of polycrystalline materials is very important in many areas, such as automotive, aerospace or energy. Various advanced approaches have been developed. However, there is still room for improvement.

The stress state is often characterised by the stress triaxiality, which describes the volumetric part of the stress tensor. It is defined as

$$\eta = \frac{\sigma_1 + \sigma_2 + \sigma_3}{3\bar{\sigma}}, \tag{1}$$

where $\sigma_1 \geq \sigma_2 \geq \sigma_3$ are the principal stresses and $\bar{\sigma}$ is the equivalent von Mises stress. The deviatoric part of the stress tensor may be described by many quantities. One of the most widespread is the normalized third invariant of deviatoric stress tensor defined as

$$\xi = \frac{27}{2}\frac{\det(\mathbf{s})}{\bar{\sigma}^3}, \tag{2}$$

where $\mathbf{s}$ is the deviatoric stress tensor (Dou et al., 2023).

The flat specimen (Fig. 2) is usually used along with other geometries for the calibration of plasticity as well as ductile fracture criteria (Park et al., 2018; Zhu et al., 2021; Nouira et al., 2023). The plane strain occurs along the width (zero strain approximately) in the centre of this specimen, while the plane stress occurs through the thickness (zero stress approximately) there. At this point, the initial values of stress triaxiality and normalized third invariant of deviatoric stress tensor are approximately 0.577 and exactly 0, which is the same case as for the tensile notched tube (Šebek et al., 2019).

* Ing. Petr Kubík, Ph.D.: Institute of Solid Mechanics, Mechatronics and Biomechanics, Faculty of Mechanical Engineering, Brno University of Technology; Technická 2896/2; 616 69, Brno; CZ, kubik.p@fme.vutbr.cz
** Ing. Radek Vobejda: Institute of Solid Mechanics, Mechatronics and Biomechanics, Faculty of Mechanical Engineering, Brno University of Technology; Technická 2896/2; 616 69, Brno; CZ, 170387@vutbr.cz
*** prof. Jindřich Petruška, CSc.: Institute of Solid Mechanics, Mechatronics and Biomechanics, Faculty of Mechanical Engineering, Brno University of Technology; Technická 2896/2; 616 69, Brno; CZ, petruska@fme.vutbr.cz
**** doc. Ing. František Šebek, Ph.D.: Institute of Solid Mechanics, Mechatronics and Biomechanics, Faculty of Mechanical Engineering, Brno University of Technology; Technická 2896/2; 616 69, Brno; CZ, sebek@fme.vutbr.cz

ISSN: 1805-8256, doi: 10.21495/em2023-143

2. Experimenting

The rolled plate of $15.875 \times 300 \times 600$ mm made from nickel-based superalloy Inconel 718 was used to manufacture the specimens. Their axes were aligned with the rolling direction estimated by metallography.

Three tensile tests of cylindrical specimens 6 mm in diameter and three tensile tests of flat plates were carried out. The flat plate has a thickness of 2.5 mm in the process zone and 10 mm in the shoulders. The width was 50 mm. All tests were carried out on the Zwick Z250 Allround-Line, tCII, testing machine with the Zwick multiXtens extensometer with a gauge length of 30 mm.

3. Numerical calculations

The constants of elasticity, Young's modulus of 202 GPa and Poisson's ratio of 0.34, were estimated on the basis of the impulse excitation measurement.

Three plasticity models were considered for the simulations. The first was the von Mises yield criterion with associated flow rule, which has no material parameter. Another one was the model proposed by Ghazali et al. (2020), which has 6 material parameters. It is dependent on the stress triaxiality and the normalized third invariant of deviatoric stress tensor. The flow rule was deviatoric associated so that the plastic incompressibility was fulfilled. It meant that the direction of flow was normal to the yield surface only in the deviatoric plane. The last plasticity model was the one proposed by Vobejda et al. (2022). It was non-associated with the yield function having 7 material parameters, the same number as the plastic potential, since it took the same form. All models were implemented using user subroutines in Abaqus/Explicit software.

The flow curve was determined on the basis of the tensile cylindrical specimen, similarly as in Šebek et al. (2019). Average experiment and simulation are compared in the left Fig. 1. The von Mises yield criterion was used. The geometry was meshed with CAX4R axisymmetric elements of size 0.075 mm.

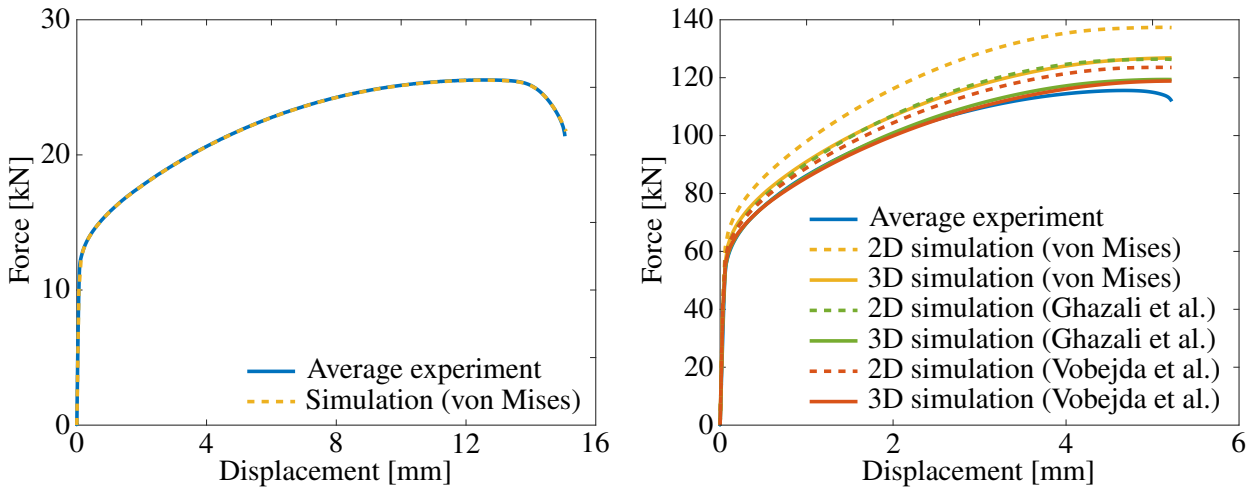

Fig. 1: Force–displacement responses for average experiments and computations for tensile cylindrical specimen (left) and tensile flat specimen modelled as plane strain, 2D, and tree-dimensionally, 3D, (right).

Two levels of modelling the flat specimen geometry were used. One eighth of three-dimensional geometry was modelled taking into consideration all planes of symmetry. The geometry was discretized by C3D8R elements with 0.075 mm size in the process zone. The mass scaling was employed in order to save some computational time. This model served for the calibration of plasticity models, except for the von Mises one. The material parameters $c_s = 0.98$ and $k_{b,y} = 0.3$ for the models of Ghazali et al. and Vobejda et al., respectively, were estimated based on the force responses. These were compared with the average experiment until a satisfactory match was reached (right Fig. 1). The other material parameters of both plasticity models remained the same as in Vobejda et al. (2022). Then, also the two-dimensional case was modelled, assuming the plane strain condition in the centre of the flat specimen (cut B – B in Fig. 2). No plane of symmetry was considered then. The geometry was meshed with CPE4R elements having again a size of 0.075 mm.

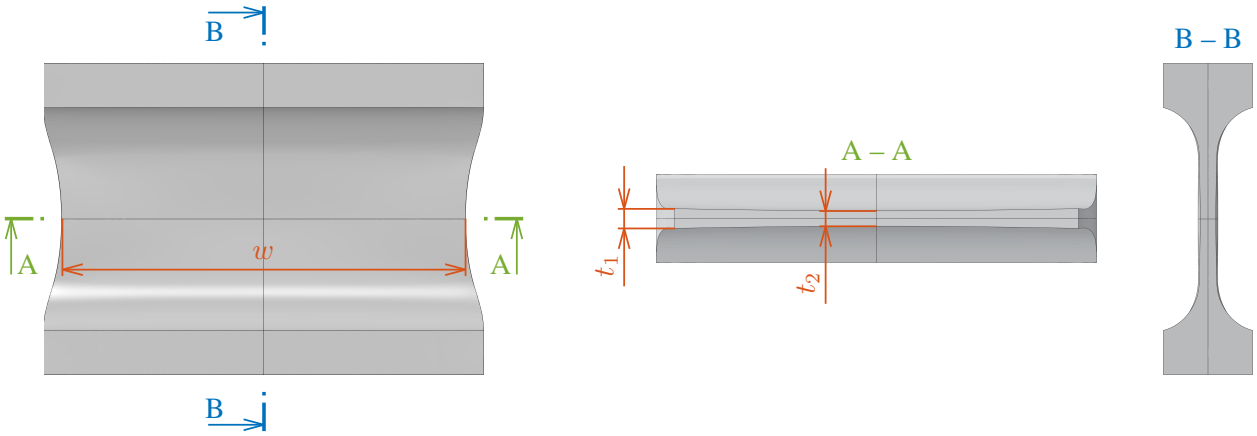

Fig. 2: Necking dimensions and cuts for the tensile flat specimen at the instant of failure.

4. Results and discussion

The force responses are comparable to the average experiment in the case of plasticity models of Ghazali et al. and Vobejda et al. for three-dimensional geometry, while the classical von Mises yield criterion overpredicted the response (right Fig. 1). Force responses were also overpredicted in the case of plane strain condition for all models of plasticity. Tab. 1 summarizes the relative errors with respect to the average experiment in order to quantify these findings.

Tab. 1: The percentage errors of plasticity models related to the average experiment.

Plasticity model	Geometry	Error [%]
Von Mises	2D	17
Von Mises	3D	7.4
Ghazali et al.	2D	7.4
Ghazali et al.	3D	1.6
Vobejda et al.	2D	5.1
Vobejda et al.	3D	1.2

The two-dimensional modelling yielded similar results for models in the view of state variables extracted from the crack initiation location (Fig. 3), consistent with the theoretical initial values. Different results were observed for the three-dimensional geometries, which should be closer to reality. The models of von Mises and Vobejda et al. predicted similar results. The average stress triaxiality was 0.327 and 0.303 for the models of von Mises and Vobejda et al., respectively, while the average normalized third invariant of deviatoric stress tensor was 0.538 and 0.540, respectively. The model of Ghazali et al. predicted the average stress triaxiality of 0.493 and the average normalized third invariant of deviatoric stress tensor of 0.609, which is almost two times higher compared to other models.

Significant necking developed before fracture in the case of a tensile flat specimen. Three neck dimensions were measured and averaged for comparison with numerical simulations (Fig. 2). Those were the width w, the thickness on the sides t_1 and the thickness on the centre t_2. The results for the three-dimensional geometry are given in Tab. 2, while the results for the two-dimensional models are given in parentheses there. The best prediction was obtained by the plasticity model proposed by Vobejda et al.

Tab. 2: Three neck dimensions for three-dimensional geometry (for two-dimensional in parentheses).

	w [mm]	t_1 [mm]	t_2 [mm]
Average experiment	46.19	2.01	1.70
Simulation (von Mises)	45.69	2.23	1.74 (1.68)
Simulation (Ghazali et al.)	47.40	2.18	1.66 (1.68)
Simulation (Vobejda et al.)	45.78	2.22	1.73 (1.69)

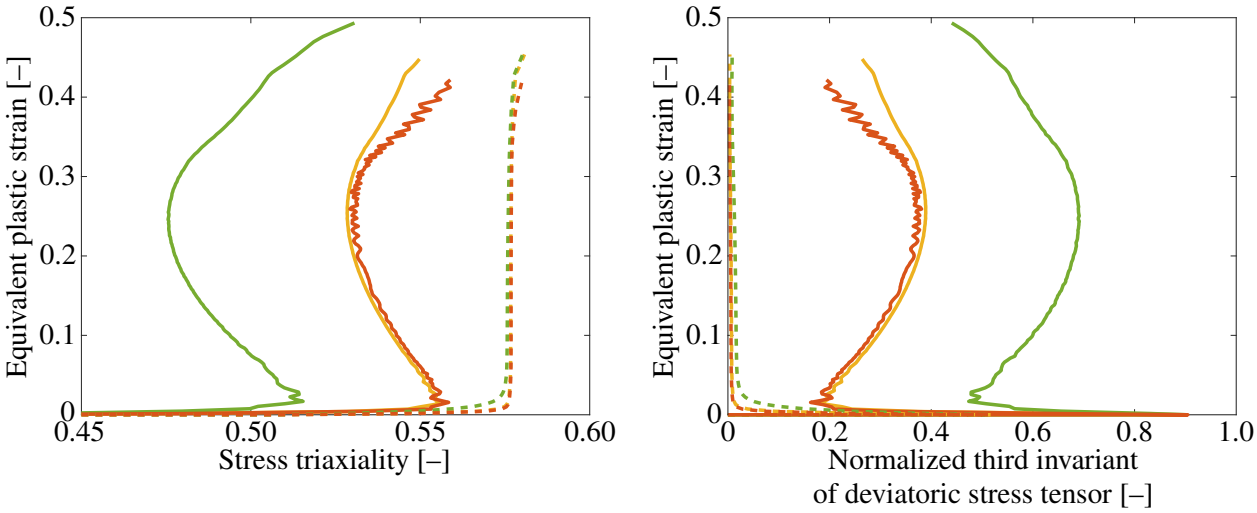

Fig. 3: State variables at centre of flat specimen (legend for simulations identical with that in right Fig. 1).

5. Conclusions

Three- and two-dimensional modelling was performed for the tensile flat specimen made from the nickel alloy Inconel 718 to see the influence of simplification. The results show that the plane strain case correctly predicted the stress state in the centre of the specimen, where the onset of the fracture occurred. On the other hand, force responses were overpredicted for all material models considered. The three-dimensional modelling brought good prediction of forces, apart from the von Mises model. However, the state variables, stress triaxiality and normalized third invariant of deviatoric stress tensor, deviated significantly for the model of Ghazali et al. with associated flow rule. The difference between predicted neck dimensions is marginal within the plasticity models considered. The non-associated model of Vobejda et al. captured the reality the closest overall.

Acknowledgments

This work is an output of the project Computational modelling of ductile fracture of identical wrought and printed metallic materials under ultra-low-cycle fatigue created with financial support from the Czech Science Foundation under the registration no. 23-04724S.

References

Dou, W., Xu, Z., Han, Y. and Huang, F. (2023) A ductile fracture model incorporating stress state effect. International Journal of Mechanical Sciences, 241, pp. 107965.

Ghazali, S., Algarni, M., Bai, Y. and Choi, Y. (2020) A study on the plasticity and fracture of the AISI 4340 steel alloy under different loading conditions and considering heat-treatment effects. International Journal of Fracture, 225(1), pp. 69–87.

Nouira, M., Oliveira, M. C., Khalfallah, A., Alves, J. L. and Menezes, L. F. (2023) Comparative fracture prediction study for two materials under a wide range of stress states using seven uncoupled models. Engineering Fracture Mechanics, 279, pp. 108952.

Park, N., Huh, H. and Jeong, W.-Y. (2018) Anisotropic fracture forming limit diagram considering non-directionality of the equi-biaxial fracture strain. International Journal of Solids and Structures, 151, pp. 181–194.

Šebek, F., Park, N., Kubík, P., Petruška, J. and Zapletal, J. (2019) Ductile fracture predictions in small punch testing of cold-rolled aluminium alloy. Engineering Fracture Mechanics, 206, pp. 509–525.

Vobejda, R., Šebek, F., Kubík, P. and Petruška, J. (2022) Solution to problems caused by associated non-quadratic yield functions with respect to the ductile fracture. International Journal of Plasticity, 154, pp. 103301.

Zhu, P., Zhang, Q., Xu, H. and Ouyang, Y. (2021) Experimental and numerical investigation on plasticity and fracture behaviors of aluminum alloy 6061-T6 extrusions. Archives of Civil and Mechanical Engineering volume, 21, pp. 88.